



ATLAS NOTE

June 28, 2011



1

Muon momentum scale from Z bosons

2

A. Kapliy, P. Onyisi, and M. Shochet

3

Univeristy of Chicago

4

Abstract

5

This note describes a data-driven method for calculating muon momentum scale factors for positive and negative muons using events with Z bosons. Muon momentum scale factors

6

are reported for the 2010 ATLAS data.

7

8	Contents	
9	1 Introduction	2
10	2 Procedure	2
11	2.1 Mathematical details	4
12	3 Z mass fit	5
13	4 Results for 2010 data	7
14	4.1 Muon selection	7
15	4.2 Relative scale R_0	7
16	4.3 Absolute scale factors k_{\pm}	7
17	5 Systematic effects	7
18	6 Applying the Results	8
19	A Systematic Uncertainty Details	11

1 Introduction

Residual misalignments in the Inner Detector (ID) and the Muon Spectrometer (MS), as well as magnetic field effects, can result in noticeable muon momentum deviations from Monte-Carlo simulation. Charge-dependent momentum scales are particularly relevant for the W charge asymmetry and ratio measurements, where muon momentum scale is an important systematic. Good understanding of MS scale is also important in various searches involving high- p_T muons, where the ID measurement contributes little to the reconstruction of a combined muon.

We define the scale factors directly on the muon *transverse momentum*, as opposed to its inverse. For brevity, we will refer to this quantity in text as simply “momentum”, even though we always mean “transverse momentum”.

$$\begin{cases} \frac{1}{p_T} \Big|_{\mu^+, \text{data}} &= \frac{1}{k_+} \frac{1}{p_T} \Big|_{\mu^+, \text{mc}} \\ \frac{1}{p_T} \Big|_{\mu^-, \text{data}} &= \frac{1}{k_-} \frac{1}{p_T} \Big|_{\mu^-, \text{mc}} \end{cases} \quad (1)$$

It is possible to arrive at charge-separated momentum scale factors by comparing the momenta of muons from W^+ and W^- decays in data with those in Monte-Carlo simulation [1]. While W bosons are substantially more abundant than Z bosons, their daughters decay with non-identical momentum distributions that depend on the charge of the boson - a feature of a proton-proton collider. Therefore, a method that relies on W bosons to derive muon momentum scale factors suffers from potential physics-related bias through Monte-Carlo modeling uncertainty (in particular, parton distribution functions). As an alternative, we develop a fully data-driven technique using Z events.

2 Procedure

By constraining the invariant mass of muons in Z candidate events to the expected Z mass, we can effectively determine the product of k_+ and k_- scale factors. Given a perfectly-aligned detector in Monte-Carlo simulation, the invariant mass scales as:

$$M_{Z|\text{data}} = M_{Z|\text{mc}} \cdot \sqrt{k_+ \cdot k_-} \quad (2)$$

Note that another equation is needed to constrain k_+ and k_- individually. It can be obtained by balancing the momenta of positive and negative muons from Z against each other.

In particular, we used Pythia $Z \rightarrow \mu\mu$ Monte-Carlo to verify that momentum spectra for tight positive and negative muons are statistically identical in the events passing standard Z selection.

$$\frac{1}{p_T} \Big|_{\mu^+, \text{mc}} = \frac{1}{p_T} \Big|_{\mu^-, \text{mc}} \quad (3)$$

By comparing the shapes of inverse p_T spectra of $Z \rightarrow \mu\mu$ muons in data, we can attribute any observed differences to detector and magnetic field effects.

The following procedure is used to obtain the ratio of k_+ to k_- , which we call the relative scale R_0 :

- Build a smooth $1/p_{T_{\mu^+}}$ kernel PDF template for positive muons (Figure 1).
- Overlay the $1/p_{T_{\mu^-}}$ spectrum on the PDF. Due to misalignments, it may not match well and will potentially result in a bad χ^2 .
- Instead, overlay $1/(R \cdot p_{T_{\mu^-}})$ spectrum for many different values of “relative” scale R (Figure 2)
- Given a plot of χ^2 vs R , fit a parabola to find $R_0 \pm \delta R_0$ at which μ^+ and μ^- spectra are compatible.

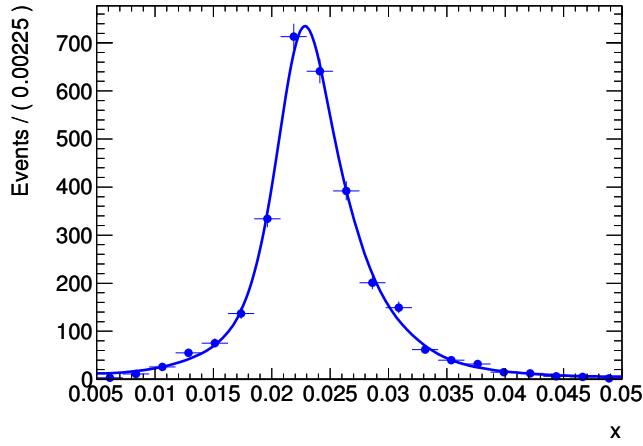


Figure 1: $1/p_T$ for μ^+ and its derived smooth PDF

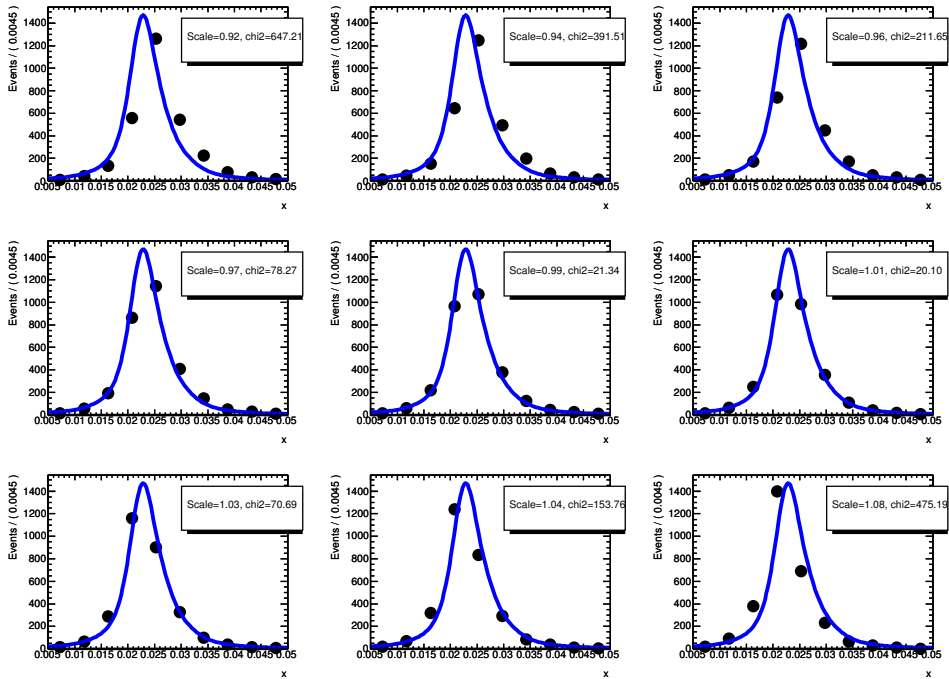


Figure 2: The $\mu^- 1/p_T$ distribution for several values of the relative scale R . The blue curve is the fixed $\mu^+ 1/p_T$ distribution.

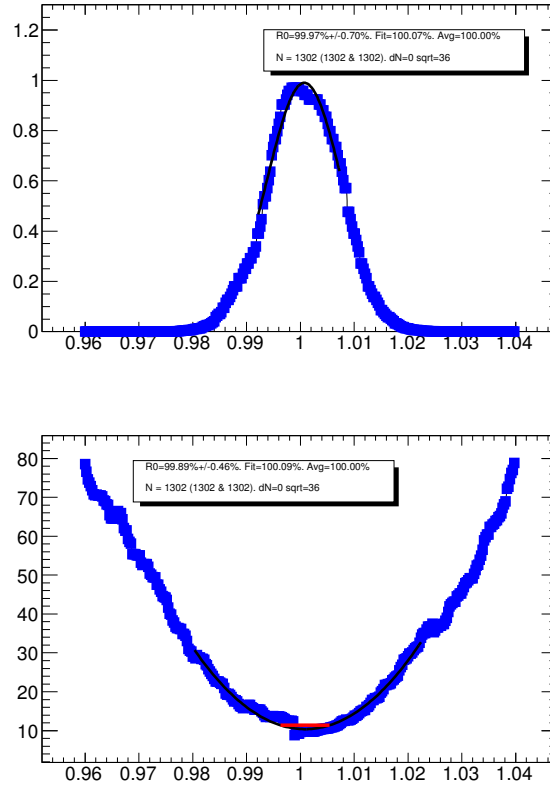


Figure 3: KS (above) and χ^2 (below) fit for the relative scale R_0 for Endcap-A combined muons. The difference between fitted peak locations obtained by these two methods is taken as a systematic.

53 As an alternative, we also perform an unbinned Kolmogorov-Smirnov (KS) test that evaluates the
 54 compatibility of $1/(R \cdot p_T)$ spectra for positive and negative muons for a range of R values. The best
 55 value, R_0 , is found when the KS probability is maximized. With large statistics, the KS and χ^2 methods
 56 yield identical results. The KS method is more robust with smaller statistics as far as the central value is
 57 concerned but doesn't provide a simple way to extract the error on the fitted parameter.

58 The χ^2 -based method requires binning the spectrum in order to calculate the χ^2 , which results in
 59 a slight loss of statistical power and introduces a systematic due to the choice of the bin size. More
 60 importantly, there is substantial freedom in the choice of the parameters used to create a kernel PDF.
 61 We investigated adaptive and non-adaptive kernels and several values of the “bandwidth” parameter
 62 (smoothing factor) and concluded that the precise location of the χ^2 minimum is somewhat sensitive to
 63 different settings but the curvature of the fitted parabola (and thus the estimate of the error on the fitted
 64 parameter) remains stable.

65 Given different relative strength of the two methods, we obtain the central value of R_0 from the KS
 66 method and the error δR_0 from the χ^2 method. Figure 3 illustrates both methods when applied to the
 67 same set of Z events.

68 2.1 Mathematical details

69 By definition of R_0 , we have:

$$\frac{1}{p_T} \Big|_{\mu_+, \text{data}} = \frac{1}{R_0} \cdot \frac{1}{p_T} \Big|_{\mu_-, \text{data}} \quad (4)$$

70 Using the definition of k_{\pm} scale factors, this becomes:

$$\frac{1}{k_+} \frac{1}{p_T} \Big|_{\mu_+, \text{mc}} = \frac{1}{R_0} \cdot \frac{1}{k_-} \frac{1}{p_T} \Big|_{\mu_-, \text{mc}} \quad (5)$$

71 Exploiting the fact that the spectra for μ_+ and μ_- are identical in Monte-Carlo, we finally obtain:

$$\frac{1}{k_+} = \frac{1}{R_0} \cdot \frac{1}{k_-} \quad (6)$$

72 Together with the previously described constraint on Z mass, we have the following system of equations:
73

$$\begin{cases} k_+ = R_0 \cdot k_- \\ M_{Z|\text{data}} = M_{Z|\text{lmc}} \cdot \sqrt{k_+ \cdot k_-} \end{cases} \quad (7)$$

74 This system can be solved for k_{\pm} :

$$\begin{cases} k_+ = \frac{M_{Z|\text{data}} \cdot \sqrt{R_0}}{M_{Z|\text{lmc}}} \\ k_- = \frac{M_{Z|\text{data}}}{M_{Z|\text{lmc}} \cdot \sqrt{R_0}} \end{cases} \quad (8)$$

75 The standard formula for error propagation yields the uncertainty on absolute scale factors. Since
76 Monte-Carlo simulation provides plenty of Z events to perform a robust mass constraint, the error on
77 $M_{Z|\text{lmc}}$ was neglected.

$$\begin{cases} \delta^2 k_+ = \delta^2(M_{Z|\text{data}}) \cdot \left(\frac{\sqrt{R_0}}{M_{Z|\text{lmc}}}\right)^2 + \delta^2(R_0) \cdot \left(\frac{M_{Z|\text{data}}}{M_{Z|\text{lmc}}}\right)^2 \cdot \frac{1}{4R_0} \\ \delta^2 k_- = \delta^2(M_{Z|\text{data}}) \cdot \left(\frac{1}{M_{Z|\text{lmc}} \cdot \sqrt{R_0}}\right)^2 + \delta^2(R_0) \cdot \left(\frac{M_{Z|\text{data}}}{M_{Z|\text{lmc}}}\right)^2 \cdot \frac{1}{4R_0^3} \end{cases} \quad (9)$$

78 3 Z mass fit

79 The Z mass constraint is applied by fitting the unbinned di-muon invariant mass spectrum to one of the
80 two functional forms described below. The location of the peak and its statistical error (as reported by
81 the fit procedure) provide M_Z and δM_Z that feed into the final calculation of k_{\pm} and their uncertainties.

82 • **Analytic Z lineshape.** Full Z lineshape including radiation and interference terms (see refer-
83 ence [2]) is convolved with a Crystal-Ball resolution model and fit in the invariant mass range
84 of 70–110 GeV. Other resolution models, such as single or double Gaussians, were investigated
85 but failed to provide adequate description of high-statistics detector-level distributions in Monte-
86 Carlo. In principle, the full lineshape fit should provide the best statistical power thanks to a wide
87 invariant mass window over which it remains applicable. Unfortunately, as a consequence of a
88 large number of free parameters, the fitting routine frequently ends up with a non positive-definite
89 error matrix, which invalidates the estimate of δM_Z .

90 • **Gaussian fit in the core.** As an alternative, we perform a Gaussian fit to the core of the invariant
91 mass distribution, which has the advantage of always converging and reporting a reliable error on
92 δM_Z . In order to avoid bias associated with the selection of an appropriate mass window around
93 the core of the distribution, the fit is performed iteratively: the first iteration obtains the width and
94 approximate position of the peak, while the second iteration fits in a one-sigma window around
95 that peak.

96 Figure 4 demonstrates that both functional forms adequately describe di-muon mass distributions in high-
97 statistics Monte-Carlo. We quote the central values for k_{\pm} obtained by the iterative Gaussian method and
98 assign a systematic uncertainty to account for the differences with respect to the full-lineshape method.

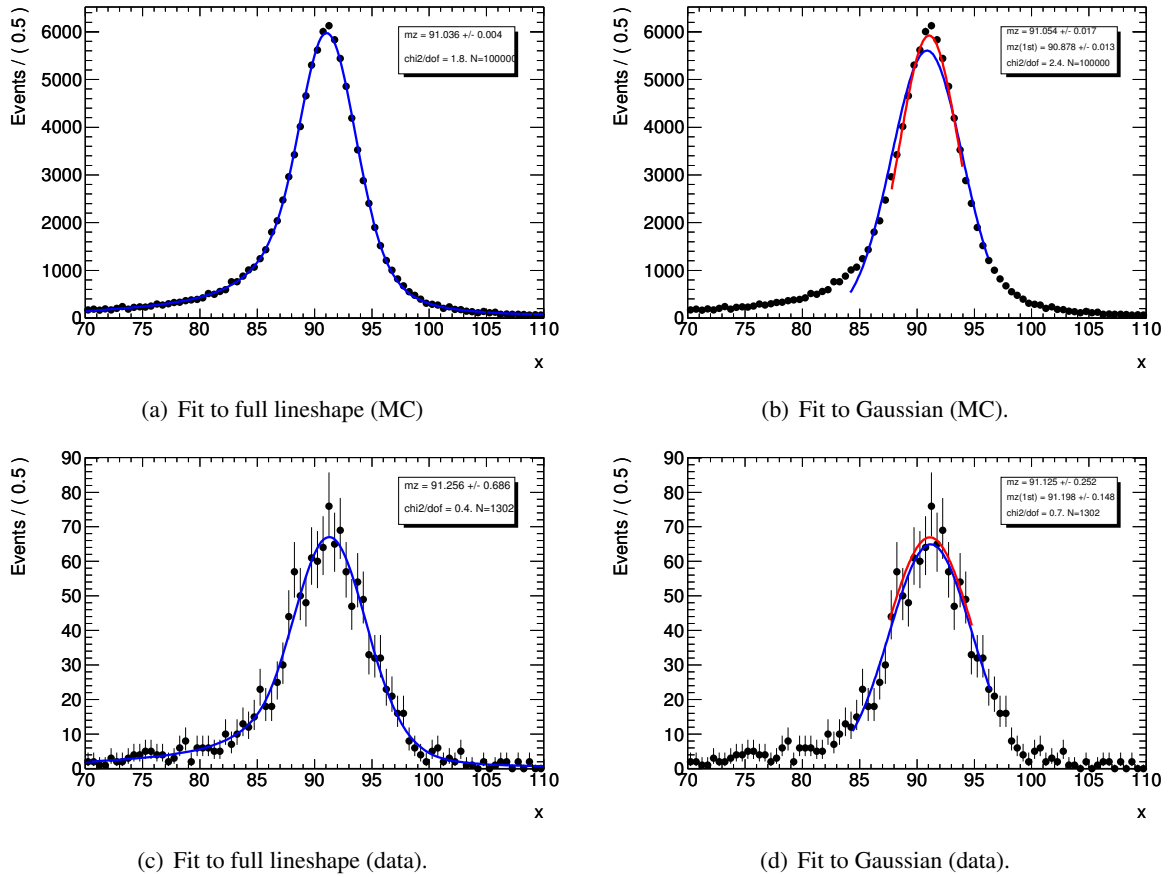


Figure 4: Z mass fits for Monte-Carlo and data events with both legs in Endcap A-side. The full lineshape consists of the analytic Z lineshape convolved with a Crystal-Ball resolution model. The gaussian fit is iteratively performed in the core of the distribution: the blue curve is the first iteration; the red curve is the final iteration.

99 4 Results for 2010 data

100 We report results for 2010 “fall reprocessing” reconstruction. Due to limited statistics in the 2010 dataset,
101 the scale factors are calculated for only three η bins: $|\eta| < 1.05$ (Barrel), $-2.4 < \eta < -1.05$ (Endcap-C),
102 and $1.05 < \eta < 2.4$ (Endcap-A).

103 4.1 Muon selection

104 The following selection requirements are imposed on muon candidates:

- 105 • They must be STACO combined muon candidates
- 106 • $|\eta| < 2.4$
- 107 • $p_T > 20$ GeV
- 108 • MCP recommendation for release 16 muon inner detector cuts [3]:
 - 109 – at least one B layer hit if one is expected
 - 110 – Number of pixel hits + number of crossed dead pixel sensors > 1
 - 111 – Number of SCT hits + number of crossed dead SCT sensors ≥ 6
 - 112 – Number of pixel holes + number of SCT holes < 2
 - 113 – Let $n_{TRThits}$ denote the number of TRT hits on the muon track, $n_{TRTOutliers}$ the number of
114 TRT outliers on the muon track, and $n \equiv n_{TRThits} + n_{TRTOutliers}$.
 - 115 * Case 1: $|\eta| < 1.9$: require $n > 5$ and $n_{TRTOutliers} < 0.9n$.
 - 116 * Case 2: $|\eta| \geq 1.9$: if $n > 5$, then require $n_{TRTOutliers} < 0.9n$.
 - 117 • Track-based isolation requiring the sum of ID transverse momenta within a cone $\Delta R < 0.4$, ex-
118 cluding the muon track, divided by the total muon transverse momentum p_T , to be less than 0.2

119 The nominal Z selection requires opposite-charge muons with an invariant mass $70 \text{ GeV} < m_{\mu\mu} < 110$
120 GeV.

121 4.2 Relative scale R_0

122 Table 1 shows the relative scale R_0 for Combined, MS, and ID muons.

123 4.3 Absolute scale factors k_{\pm}

124 Table 2 shows the absolute scale factors k_{\pm} for combined, MS, and ID muons.

125 5 Systematic effects

126 The following systematic effects are associated with the procedure that determines the relative scale R_0 :

- 127 • **Expanded sample** (Table 5 in the Appendix). Given a particular η range for which we want to
128 compute the relative scale, we have two ways of choosing a subset of appropriate Z events. We
129 can require that both Z legs fall in that particular η region, or we can make no such requirement and
130 include events where the leg with the opposite charge falls anywhere within the fiducial η region.
131 The difference between the results for the nominal and extended samples is taken as a systematic
132 uncertainty.

Region	R_0	δR_0
Combined muons		
Endcap-A	100.1%	0.5%
Barrel	100.3%	0.4%
Endcap-C	101.7%	0.5%
MS muons		
Endcap-A	101.1%	0.6%
Barrel	100.4%	0.4%
Endcap-C	98.0%	0.6%
ID muons		
Endcap-A	99.9%	0.4%
Barrel	100.2%	0.4%
Endcap-C	102.7%	0.6%

Table 1: Relative scales in 2010 data

- **Mass window for Z selection** (Table 6 in the Appendix). The window around the nominal Z mass was reduced from 70–110 GeV to 80–100 GeV, which changed the composition of the Z sample used to determine R_0 . The difference between the results for the nominal and reduced windows is taken as a systematic uncertainty.
- **Shape comparison method** (Table 7 in the Appendix). As described earlier, we employ two alternative techniques (χ^2 and KS) to arrive at the relative scale R_0 . The difference between the two methods is taken as a systematic uncertainty.

The following systematic effect is associated with the invariant mass constraint and happens after R_0 has already been determined:

- **Z mass fit function** (Table 8 in the Appendix). Instead of using a Gaussian fit in the core, we also performed a full Z lineshape fit with a Crystal-Ball resolution function. Because the fit in the data is normalized to the corresponding fit in the Monte-Carlo, any systematic shifts introduced by either method are cancelled in the ratio. The difference in the results of the two methods is taken as a systematic uncertainty.

6 Applying the Results

We provide central values for the scales k_+ and k_- (Table 2), as well as the fully correlated and anticorrelated uncertainties on these values (Table 3). These corrections are valid for muons in the approximate p_T range 20–50 GeV. To apply these corrections to Monte-Carlo events, μ^+ and μ^- candidates should have their p_T multiplied by k_+ and k_- respectively for the appropriate muon type and η region. We factor the uncertainty in the scale measurements into correlated and anticorrelated components, where correlated means that the quantity k_+/k_- is kept constant (the scales for both charges change in the same direction), and anticorrelated means that k_+k_- is kept constant (the scales change in opposite directions). Note that the correlated and anticorrelated uncertainties are uncorrelated between η regions and between different types of muons. The effects of the correlated and anticorrelated terms should be evaluated separately and then added in quadrature to obtain an overall uncertainty due to momentum scale.

We also provide the deviations observed in the scales when we use smaller η bins (Table 4). This gives a measure of how much structure in k_{\pm} is hidden by our averages over large η regions. Note that

Region	k_+	k_-
Combined muons		
Endcap-A	$100.12 \pm 0.36\%$	$100.04 \pm 0.36\%$
Barrel	$100.09 \pm 0.21\%$	$99.81 \pm 0.21\%$
Endcap-C	$100.94 \pm 0.35\%$	$99.23 \pm 0.34\%$
MS muons		
Endcap-A	$100.02 \pm 0.48\%$	$98.93 \pm 0.48\%$
Barrel	$100.09 \pm 0.26\%$	$99.74 \pm 0.26\%$
Endcap-C	$99.06 \pm 0.49\%$	$101.14 \pm 0.50\%$
ID muons		
Endcap-A	$100.05 \pm 0.44\%$	$100.17 \pm 0.44\%$
Barrel	$99.78 \pm 0.21\%$	$99.60 \pm 0.21\%$
Endcap-C	$101.56 \pm 0.39\%$	$98.92 \pm 0.38\%$

Table 2: Absolute scale factors in 2010 data. Only statistical uncertainty is shown.

	Combined			MS only			ID only		
	EA	B	EC	EA	B	EC	EA	B	EC
Statistical Uncertainties									
R_0 determination	0.23	0.18	0.25	0.30	0.20	0.30	0.22	0.18	0.27
Z mass	0.28	0.11	0.25	0.38	0.17	0.40	0.39	0.10	0.28
Systematic Uncertainties									
Expanded sample	0.04	0.38	0.04	0.02	0.42	0.64	0.14	0.31	0.06
Mass window for Z selection	0.04	0.02	0.13	0.16	0.05	0.45	0.06	0.02	0.08
Shape comparison method	0.00	0.12	0.36	0.06	0.07	0.19	0.10	0.14	0.18
Z mass fit function	0.17	0.09	0.03	0.34	0.03	0.09	0.26	0.09	0.13
Summary									
Correlated (constant k_+/k_-)	0.32	0.14	0.25	0.51	0.17	0.41	0.46	0.13	0.31
Anti-correlated (constant k_+k_-)	0.23	0.44	0.45	0.35	0.47	0.86	0.29	0.39	0.34

Table 3: Summary of uncertainties on k_{\pm} by region and muon type.

160 only relative scales R_0 were recalculated in smaller η bins and propagated to absolute scale factors k_{\pm} .
 161 The Z mass constraint is still applied on the wider η bins to ensure sufficient statistics. We caution that
 162 there can still be significant unresolved structure in ϕ and η and so these results should *not* be taken as
 163 limits on the momentum scale deviation on a per-muon basis.

Region	Δk_+	Δk_-	δk_{\pm}
Combined muons			
Endcap A-side ($2.0 < \eta < 2.4$)	-1.14%	1.15%	0.42%
Endcap A-side ($1.05 < \eta < 2.0$)	0.32%	-0.31%	0.22%
Barrel A-side ($0.0 < \eta < 1.05$)	-0.21%	0.21%	0.12%
Barrel C-side ($-1.05 < \eta < 0.0$)	0.19%	-0.19%	0.19%
Endcap C-side ($-2.0 < \eta < -1.05$)	-0.35%	0.35%	0.19%
Endcap C-side ($-2.4 < \eta < -2.0$)	1.23%	-1.19%	0.32%
MS muons			
Endcap A-side ($2.0 < \eta < 2.4$)	-0.07%	0.07%	0.48%
Endcap A-side ($1.05 < \eta < 2.0$)	-0.02%	0.02%	0.23%
Barrel A-side ($0.0 < \eta < 1.05$)	-0.06%	0.06%	0.08%
Barrel C-side ($-1.05 < \eta < 0.0$)	0.09%	-0.10%	0.24%
Endcap C-side ($-2.0 < \eta < -1.05$)	-0.35%	0.35%	0.33%
Endcap C-side ($-2.4 < \eta < -2.0$)	0.55%	-0.55%	0.58%
ID muons			
Endcap A-side ($2.0 < \eta < 2.4$)	-2.00%	2.04%	0.59%
Endcap A-side ($1.05 < \eta < 2.0$)	0.62%	-0.61%	0.04%
Barrel A-side ($0.0 < \eta < 1.05$)	-0.33%	0.33%	0.20%
Barrel C-side ($-1.05 < \eta < 0.0$)	0.37%	-0.37%	0.19%
Endcap C-side ($-2.0 < \eta < -1.05$)	-0.43%	0.42%	0.14%
Endcap C-side ($-2.4 < \eta < -2.0$)	1.83%	-1.75%	0.41%

Table 4: Deviations of scale factors in smaller η bins from those given in Table 2. The last column represents *additional* statistical uncertainty due to the fact that the relative scales were computed in a narrower η bin: $\sqrt{\delta k_{\pm}^2|_{narrow} - \delta k_{\pm}^2|_{wide}}$. Due to lower statistics available in narrow η bins, all numbers in this table carry a larger systematic uncertainty than those presented for the wide- η case.

164 **A Systematic Uncertainty Details**

Region	Δk_+	Δk_-
Combined muons		
Endcap-A	+0.04%	-0.04%
Barrel	-0.38%	+0.38%
Endcap-C	+0.04%	-0.04%
MS muons		
Endcap-A	-0.02%	+0.02%
Barrel	-0.42%	+0.42%
Endcap-C	+0.63%	-0.64%
ID muons		
Endcap-A	+0.14%	-0.14%
Barrel	-0.31%	+0.31%
Endcap-C	-0.06%	+0.05%

Table 5: Systematic change in k_{\pm} when one of the Z legs is allowed to be outside of the fiducial region, expanding the sample size used in R_0 determination.

Region	Δk_+	Δk_-
Combined muons		
Endcap-A	-0.04%	+0.04%
Barrel	-0.02%	+0.02%
Endcap-C	-0.13%	+0.12%
MS muons		
Endcap-A	-0.16%	+0.16%
Barrel	+0.05%	-0.05%
Endcap-C	+0.44%	-0.45%
ID muons		
Endcap-A	-0.06%	+0.06%
Barrel	+0.02%	-0.02%
Endcap-C	-0.08%	+0.08%

Table 6: Systematic change in k_{\pm} associated with a reduction of the mass window used in the R_0 fit procedure from 70–110 GeV to 80–100 GeV.

Region	Δk_+	Δk_-
Combined muons		
Endcap-A	+0.00%	-0.00%
Barrel	-0.12%	+0.12%
Endcap-C	-0.36%	+0.35%
MS muons		
Endcap-A	+0.06%	-0.06%
Barrel	-0.07%	+0.07%
Endcap-C	-0.19%	+0.19%
ID muons		
Endcap-A	-0.10%	+0.10%
Barrel	-0.14%	+0.14%
Endcap-C	-0.18%	+0.17%

Table 7: Systematic change in k_{\pm} associated with the difference between the χ^2 and KS methods of finding R_0

Region	Δk_+	Δk_-
Combined muons		
Endcap-A	+0.17%	+0.16%
Barrel	-0.09%	-0.09%
Endcap-C	+0.03%	+0.03%
MS muons		
Endcap-A	+0.34%	+0.34%
Barrel	-0.03%	-0.03%
Endcap-C	+0.09%	+0.09%
ID muons		
Endcap-A	-0.26%	-0.26%
Barrel	+0.09%	+0.09%
Endcap-C	-0.13%	-0.13%

Table 8: Systematic change in k_{\pm} when the fit function is changed from simple Gaussian to full Z line-shape.

165 **References**

- 166 [1] J. Barreiro Guimaraes da Costa et al., *Measurement of $W \rightarrow \mu\nu$ charge asymmetry in proton-proton*
167 *collisions at $\sqrt{s} = 7$ TeV with the ATLAS detector*, ATL-COM-PHYS-2011-099, available from
168 <http://cdsweb.cern.ch/record/1326627>.
- 169 [2] A. Collaboration, *Muon Momentum Resolution in First Pass Reconstruction of pp Collision Data*
170 *Recorded by ATLAS in 2010*, ATLAS-CONF-2011-046, available from
171 <http://cdsweb.cern.ch/record/1338575>.
- 172 [3] Muon Combined Performance Group, *Guidelines for Analysis in Release 16*,
173 <https://twiki.cern.ch/twiki/bin/view/AtlasProtected/MCPAnalysisGuidelinesRel16>.